

## DISCRETE MECHANISM DAMPING EFFECTS IN THE SOLAR ARRAY FLIGHT EXPERIMENT

E. D. Pinson<sup>\*</sup>

Accelerometer data were collected during on-orbit structural dynamic testing of the Solar Array Flight Experiment aboard the Space Shuttle, and were analyzed at Lockheed Missiles and Space Co. to determine the amount of damping present in the structure. The results of this analysis indicated that the damping present in the fundamental in-plane mode of the structure substantially exceeded that of the fundamental out-of-plane mode. In an effort to determine the source of the higher in-plane damping, a test was performed involving a small device known as a constant-force spring motor or constant-torque mechanism. Results from this test indicate that this discrete device is at least partially responsible for the increased in-plane modal damping of the Solar Array Flight Experiment structure.

INTRODUCTION

A common feature of large, lightweight, flexible structures is the dominant, and typically very low-frequency, first vibrational mode. Since most of the vibrational energy of these and other types of structures tends to be concentrated in the first mode, the amplitude of oscillations at the corresponding frequency can be relatively large. In situations where this is a problem, strategically placed damping devices and/or materials can help to reduce the magnitude of the ensuing motions.

In the design of the Solar Array Flight Experiment (SAFE), a small device known as a constant-torque mechanism (CTM) was found to be effective in damping certain motions of the structure. The devices were not installed in the experiment for this purpose, but their effect on the fundamental in-plane vibrational mode of the SAFE is evident when comparing the damping factors obtained from the analysis of accelerometer data. The damping characteristics of these mechanisms are further demonstrated by the test described in this report.

SAFE BACKGROUND INFORMATION AND HARDWARE DESCRIPTION

The National Aeronautics and Space Administration (NASA) launched Space Shuttle mission STS-41-D on August 31, 1984. One of the goals of this mission was to deploy and perform various tests on the SAFE which would both verify and improve present methods of dynamic response prediction for

<sup>\*</sup>Lockheed Missiles & Space Company, Sunnyvale, California.

large, lightweight, flexible structures. Pursuant to this goal, two finite-element (FE) models of the deployed SAFE "wing" were formulated at Lockheed Missiles and Space Co. (LMSC). One model simulates the wing at 70% extension while the other simulates full deployment of the array. Both models were constructed using the EAL/SPAR FE code and were used both before and after on-orbit testing to obtain natural frequencies and mode shapes as well as simulate transient response of the SAFE structure during several excitation scenarios.

The SAFE structure (see Figure 1) was designed and integrated at LMSC in Sunnyvale, CA under contract to Marshall Space Flight Center (MSFC) in Huntsville, AL (contract number NAS8-31352). The mast assembly, produced by Able Engineering Company, Inc. of Goleta, CA, incorporates a canister deployment mechanism which allows the entire mast length of 32 m (105 ft.) to be coiled into a cylinder 1.5 m (5 ft.) long. The triangular mast, only 36 cm (14.4 in.) in circumscribed diameter, can be deployed/retracted at a nominal rate of 4 cm/sec. (1.5 in./sec.) and has an effective EI of  $43.6 \text{ kN-m}^2$  ( $15.2 \times 10^6 \text{ lbs-in}^2$ ).

The solar array blanket weighs 1.35 kN (303 lbs.) and consists of 84 rectangular panels each 4 m (13.125 ft.) by 37 cm (14.49 in.) and structurally capable of supporting solar cells. However, only one of these panels, located near the top of the blanket, was populated with active solar cells during on-orbit testing - all others were fitted with aluminum plates simulating the thickness and mass of solar cells. The panel which contained active solar cells was constructed of two 25.4 micro-meter (1.0 mil) Kapton substrates with copper circuitry sandwiched between. Five of the panels were stiffened by a graphite-epoxy framework (all others were stiffened by an aluminum framework) and joined to adjacent panels along the longest sides utilizing an s-glass rod which formed the rib of a "piano-hinge" construction. Small springs were placed at discrete points along the hinge-line to guarantee that the panels would fold in the proper directions during retraction. Although they have little effect in a 1-g environment, these springs were quite effective during the on-orbit tests.

During launch and landing, the blanket was folded into a containment box which exerted a compressive force of 13.3 kN (3000 lbs.) on the 9 cm (3.5 in.) stack of panels. The entire jettisonable structure (including the canister, mast and blanket) weighs approximately 3 kN (673 lbs.) - one-third the weight of conventional solar arrays.

The SAFE wing was designed to function at full and 70% deployment. During full deployment, approximately 23.1 N (5 lbs.) of tensile force was applied to the lower edge of the blanket through springs attached to a tension bar and then to two parallel tension wires. Additionally, a similar apparatus applied approximately 55.6 N (12.5 lbs.) to the upper 70% of the blanket. During 70% deployment, only the latter tensioning system was used. The forces transmitted through the tension bars were regulated by two separate pairs of CTMs which were designed to provide constant tension on the blanket during all structural motions. To guide and lightly hold the

position of the blanket, three stainless-steel guide-wires, placed in the middle and to either side of the centerline of the blanket, were connected to the containment box lid, laced through eyelets in the blanket, and connected to three separate CTMs in the containment box. Each of these CTMs applied approximately 8.9 N (2 lbs.) tension to the guide-wires.

#### DESCRIPTION OF THE CONSTANT-TORQUE MECHANISMS

In general, CTMs consist of three component parts:

1. A take-up drum or reel,
2. One or more thin, flat spring bands, and
3. An equal number of spring storage drums.

The take-up drum is typically divided into two segments - one reserved for the tension-wire or band and the other reserved for the constant-force spring(s). Usually, this reel is placed between two or more spring storage drums, although one such drum could be used. The constant-force springs are manufactured with an inherent tendency to coil at a certain natural radius ( $R_N$ ). This natural radius should be slightly smaller than the radius of the spring storage drum and approximately 50% smaller than the spring segment of the take-up drum, according to current design practice. In the SAFE design, at zero deployment of the tension-wire, the constant-force springs are wound almost completely around the storage drums. As the tension-wire deploys, the springs wind around the take-up drum in a direction opposite to that in which they were stored.

The amount of force applied to the tension-wire is dependent on the number of and size of the constant-force springs, and the relative diameters of the two segments of the take-up drum - the spring segment and the tension-wire segment (see Figures 2 and 3). Ideally, constant-force springs of the same cross-section, material, and natural radius should supply identical torques to the spring-segment of the take-up drum, which provides tension to the tension-wire (with the moment arm equal to the radius of the tension-wire segment). The force in the tension-wire due to one CTM is thus given by the following equation (the contributions of several CTMs may be superimposed):

$$T_T = \frac{Ebt^3}{26R_S R_T} (r + 1)^2 \quad (1)$$

where:  $T_T$  = Tension in the tension-wire,  
 $E$  = Modulus of elasticity of the spring material,  
 $b$  = Width of the spring,  
 $t$  = Thickness of the spring,  
 $R_T$  = Radius of the tension-wire segment of the take-up drum,  
 $R_N$  = Natural radius of curvature of the spring,  
 $R_S$  = Radius of the spring segment of the take-up drum, and  
 $r = R_S/R_N$ .

Figure 2 shows the locations of all but one of the CTMs used in the SAFE relative to the centerline of the containment box. (The CTM regulating tension in the center guide-wire is not shown, but is identical to the other guide-wire CTMs.) As noted in this figure and discussed above, the inner CTM regulates the tension applied to the upper 70% of the solar array blanket. Adjacent to this mechanism, is the device which supplies tension to the lower tension bar, and farthest outboard is the CTM regulating the force applied to the lid of the containment box. Although the width of the springs in the outboard CTM is considerably smaller than the other two, several qualitative observations may be made: Notice the relative number of spring storage drums for each of the three mechanisms. The inboard device, supplying the most force, has five constant-force springs acting in concert while the other two, each supplying considerably less force, have fewer springs connected to them. Note also the relative diameters of the two segments of the take-up drums (labeled on only the outboard mechanism).

#### SAFE DAMPING FACTORS AND PRELIMINARY INVESTIGATIONS

As mentioned earlier, accelerometer data that was obtained during on-orbit structural dynamic testing was analyzed at LMSC to determine various characteristics of the SAFE. One of the explicit goals of this analysis was to determine the modal damping factors applicable to the structure. The on-orbit tests were divided into three categories: out-of-plane (O/P), in-plane (I/P), and multi-modal (M/M). Several tests from each of these categories were performed at 70% deployment of the SAFE, but only one O/P and one M/M test was performed at full deployment. A total of fourteen such tests were performed, some during orbital night and some during orbital daytime. Details regarding the performance of these tests and the subsequent accelerometer data analysis are contained in Reference 1 and are not included in this report. However, a summary of the average damping factors resulting from this analysis is contained in Table 1.

In this table, the reader will notice a small difference in modal damping factors between orbital night and daytime, a large difference in all modal damping factors between 70% and 100% deployment, and a large difference between the fundamental O/P and I/P modal damping factors (i. e., the first and second modes of the structure, respectively) for all test categories. Damping differences due to thermal effects (orbital night and daytime) are well known and documented for most engineering materials, therefore this difference was somewhat expected. The modal damping factor differences between 70% and 100% deployment are not fully understood as yet, but may be attributable to the larger structural displacements (and hence more "slip" than "stick" in joint motions) at full deployment. The remaining difference, evident in Table 1, and the subject of this paper, is the difference in damping factors between I/P and O/P modes.

Upon close inspection of the table, it is seen that the ratio between the I/P and O/P modal damping factors for any given category of test (i. e., daytime, 70% deployment) is consistently greater than 1 and rarely below 2. (The obvious, and unexplained, exception to this rule is seen in the

results of the analysis of file 10.) This fact leads the analyst to conclude that a basic and relatively constant difference between I/P and O/P motions of the SAFE structure is responsible for the observed differences in modal damping factors. Intuitively, one such difference, which was later verified by transient response analyses, is the greater participation of all CTMs during I/P motions of the array. Results from these analyses show that, during I/P tests, the lower corners of the blanket oscillated along the mast axis at approximately ten times the amplitude observed during O/P tests. Since the lower edge of the blanket was attached to one of the two tension bars during all tests performed and the motions of the tension bars were regulated by one of two CTM pairs, the devices were ten times more active during I/P tests than they were during O/P tests. Other differences between I/P and O/P motions, such as twisting of the mast, do not exhibit the same dramatic participation changes and are thus assumed to have less impact on overall modal damping factors.

In order to determine whether the CTMs could indeed be responsible for the additional damping in the fundamental I/P mode, several calculations were performed. The maximum kinetic energy of the structure was over-estimated by a rigid body motion similar to the structural mode in question. In performing this calcul. the following assumptions were made:

1. The blanket was modeled as a rigid, rectangular plate of the appropriate dimensions and mass,
2. The mast was modeled as a rigid, slender rod of the appropriate dimensions and mass, coupled to the blanket during all I/P motions - a conservative assumption,
3. The blanket-mast composite body was assumed to be hinged at the at the base, making it free to rotate in the I/P direction - a conservative assumption, and
4. The angular rate at which the composite body was assumed to rotate was calculated by multiplying the maximum I/P amplitude by the natural frequency of this mode - a conservative assumption. (This method is analogous to determining the velocity of a single degree-of-freedom oscillator.)

In actuality, the mast is not hinged at the base and motions of the mast and blanket are coupled only at the mast tip. Further, the SAFE structure is not a single degree-of-freedom system (i. e., all of the mass does not participate equally in the fundamental I/P mode). However, in spite of the overly conservative assumptions, the kinetic energy was estimated to be only 0.4 J (0.39 in-lbs).

Next, the assumption was made that the kinetic energy estimated above would be totally dissipated in one cycle of oscillation. This was further assumed to be accomplished solely by a force imbalance between the two guide-wires which were attached to opposite ends of the containment box lid and tethered to the outboard CTMs. Under these constraints, a force imbalance (i. e., the difference in force applied by the CTM during deployment and retraction) of only 3.4 N (0.8 lbs.) would be required. Since the force imbalance required was so small, a test was devised to measure the actual force hysteresis.

## CONSTANT-TORQUE MECHANISM TEST DESCRIPTION

In an effort to accurately characterize the subtle force differences that were possibly inherent in the guide-wire CTM, the test plan contained in Reference 2 was devised. The plan required that two access panels be removed prior to re-routing the guide-wire around the guide-wire pulley which is detailed in Figure 5. This was done to avoid the effects of friction between the guide-wire and the SAFE blanket grommets and containment box orifices through which the guide-wire passed during on-orbit testing. Further, this allowed the test apparatus to be placed conveniently underneath the SAFE hardware. A comparison between the operational and test configuration routes of the guide-wire is presented in Figure 6.

The end of the re-routed guide-wire, connected to the containment box lid during on-orbit testing, was attached to a load cell. The load cell was then connected to a pulley which was offset from the shaft of an electric drive motor. Photographs, taken prior to the test, of the outboard CTM mounted in the SAFE and the test configuration are presented in Figures 7 and 8, respectively.

Prior to performing the test, the load cell was calibrated to register the nominal 8.9 N (2 lbs.) to within 0.2 N (0.05 lbs.) during operation of the motor. This accuracy was also verified in increments of 0.2 N (0.05 lbs.) up to a maximum of 11.1 N (2.5 lbs.). During the test, which was performed at standard temperature and pressure in an LMSC building, the motor cycled at a nominal speed of 1 r.p.m., the pulley offset was varied from 0.64 cm (0.25 in.) to 2.54 cm (1 in.), and force hysteresis was measured at four deployment positions (zero, 35%, 70%, and 100%). Early test results indicated that the force hysteresis was relatively insensitive to variations in the pulley offset, therefore during most of the time when measurements were recorded, the pulley was offset from the motor shaft a distance of 2.54 cm (1 in.).

## CONCLUSIONS AND IMPLICATIONS

Results of the CTM damping test, presented in Table 2, show that a definite force hysteresis exists. Further, the magnitude of the variation in force supplied to the guide-wire is large enough to account for most, if not all, of the added damping found in the fundamental I/P mode of the SAFE based on the approximate calculations presented in this report. The fact that these mechanisms are able to provide such relatively large levels of damping is both surprising and encouraging: With the advent of large, lightweight space structures, and the associated structural dynamic problems, the relatively simple CTMs may find a new range of application as discrete damping devices. It is suggested that further research be done to enhance the capabilities of these devices to provide predictable levels of modal damping to other space structures, such as trusses and antennas.

## ACKNOWLEDGEMENTS

The FE element model of the SAFE, an indispensable tool during these investigations, was constructed by B. A. Simpson and modified by T. J. Venator and E. D. Pinson (all employed by LMSC, Structural Dynamics). The author wishes to thank M. D. Menning (LMSC, Solar Array Projects) for his generous contributions, both technical and organizational during the preparation of this report. Appreciation is also due to the SAFE program office at MSFC for allowing LMSC to perform this and other tests involving the SAFE hardware.

## REFERENCES

1. Damping Characteristics of the Solar Array Flight Experiment, by E. D. Pinson, paper presented at the Vibration Damping Workshop II held in Las Vegas, Nevada, March 5-7, 1986.
2. Procedure for SAFE Post Flight ... (CTM) ... Test, by M. D. Menning, LMSC Doc. Number F027194, approved August 9, 1985.

Table 1: Modal Damping Values for the SAFE Structure Observed by Accelerometer Data Analysis Performed at LMSC (Abridged Listing)

File	Day/Night	Type	Modal Damping [% of critical]	
			Mode 1 (O/P)	Mode 2 (I/P)
5	Daytime	O/P, 70%	3.0	N/A <sup>1</sup>
6	Nighttime	O/P, 70%	6.0/9.0 <sup>2</sup>	N/A
10	Daytime	M/M, 70%	7.0	8.0
11	Nighttime	M/M, 70%	3.0	11.0
12	Daytime	O/P, 70%	4.5	N/A
13	Nighttime	I/P, 70%	N/A	11.0
14	Daytime	M/M, 70%	4.5	11.0
15	Nighttime	M/M, 70%	4.5	11.0
17	Daytime	O/P, 100%	2.0	N/A
20	Daytime	M/M, 100%	2.0	4.0
26	Nighttime	M/M, 70%	6.0	11.0
27	Daytime	M/M, 70%	3.0	9.0
28	Nighttime	I/P, 70%	N/A	15.0
29	Daytime	I/P, 70%	N/A	11.0
Avg.	Daytime	70%	4.4	9.8
Avg.	Nighttime	70%	5.1	11.8
Avg.	Daytime	100%	2.0	4.0

### NOTES:

1. N/A denotes that the test performed was not intended to measure the damping present in that mode.
2. The damping values given for file 6 represent values observed when a) zero initial conditions were assumed, and b) modal initial conditions were approximated in the transient response analysis, respectively.
3. Files 26, 27, 28, and 29 represent tests having a longer excitation duration than the others that are listed in this table.

Table 2: CTM Force Hysteresis Test Results

	% SAFE Deployment / Pulley Offset [in]				
	0 / 0.5	0 / 1.0	35 / 1.0	70 / 1.0	100 / 1.0
Force Hysteresis <sup>1</sup> [pounds]	0.62	0.66	0.62	0.74 <sup>2</sup>	0.68

NOTES:

1. Force hysteresis was determined by subtracting the tensile force in the guide-wire during retraction from the tension in the wire during extension.
2. The force hysteresis value presented for 70% SAFE deployment is the average of three hysteresis values obtained during separate tests at this position.

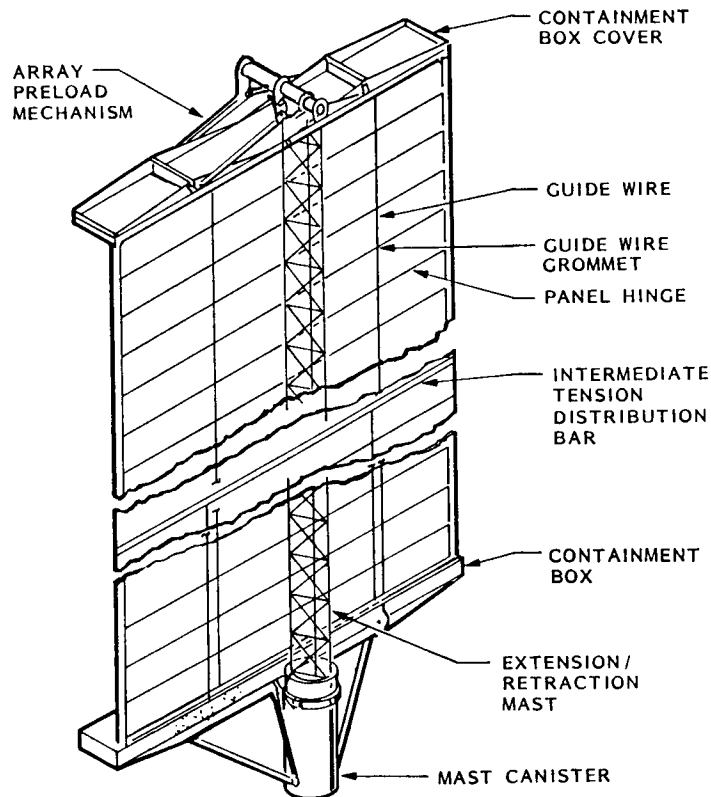


Figure 1. - SAFE hardware components.



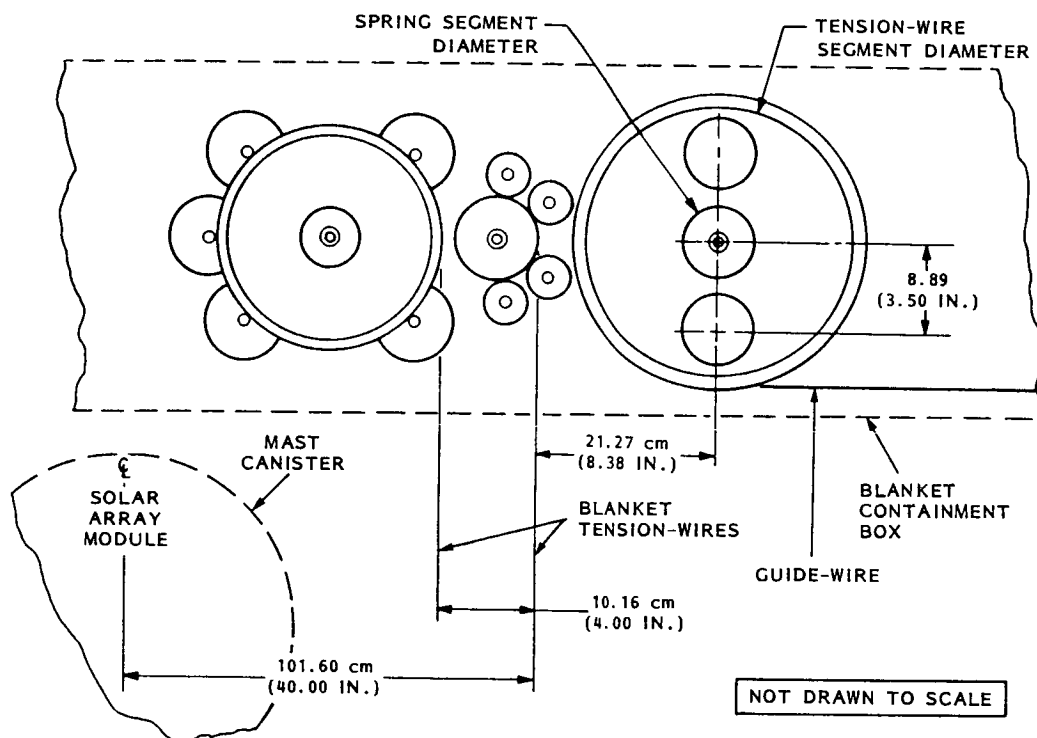


Figure 2. - Guide-wire and blanket tensioning mechanisms.

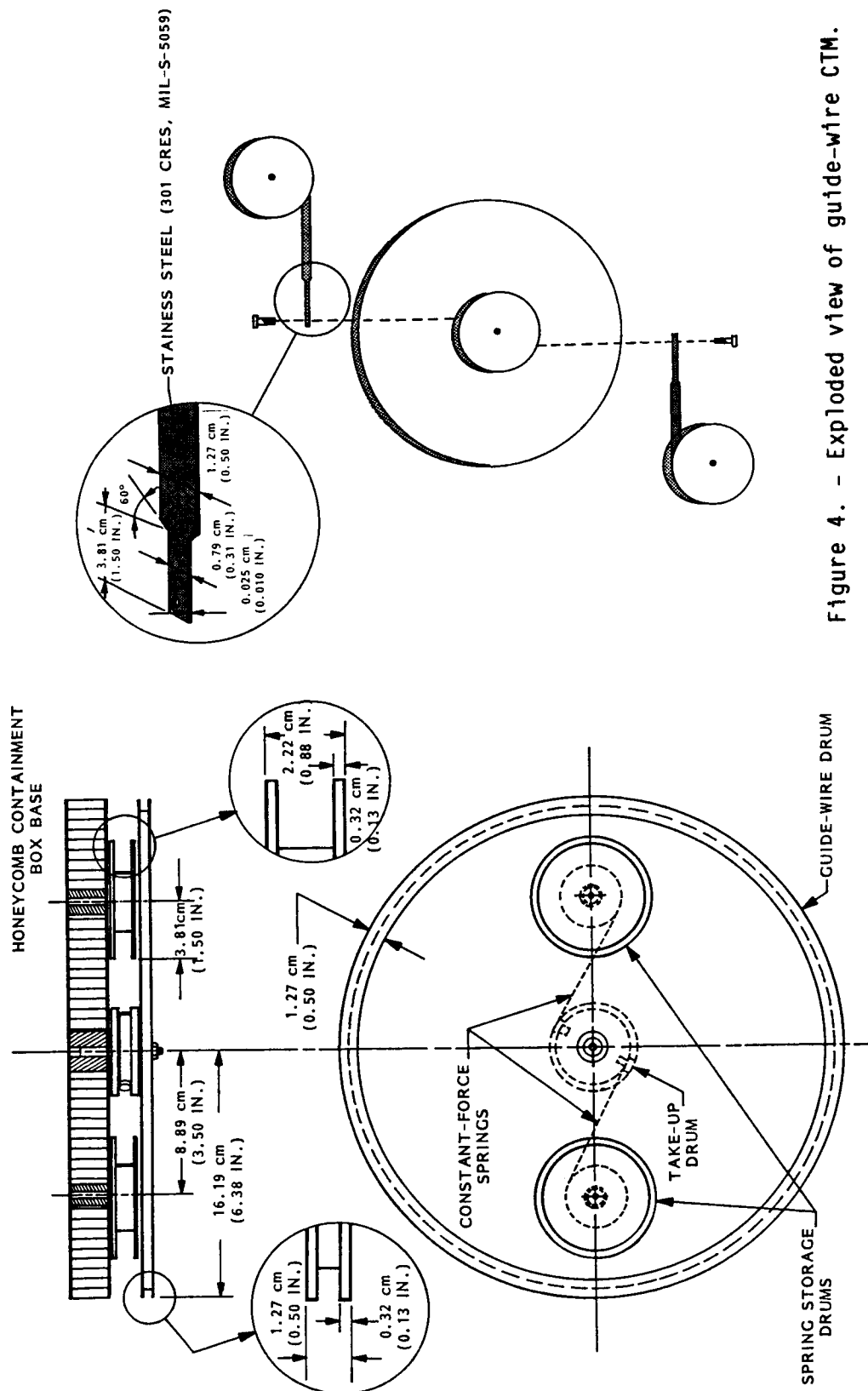


Figure 3. - Design details of guide-wire CTM.

Figure 4. - Exploded view of guide-wire CTM.

ORIGINAL PAGE IS  
OF POOR QUALITY

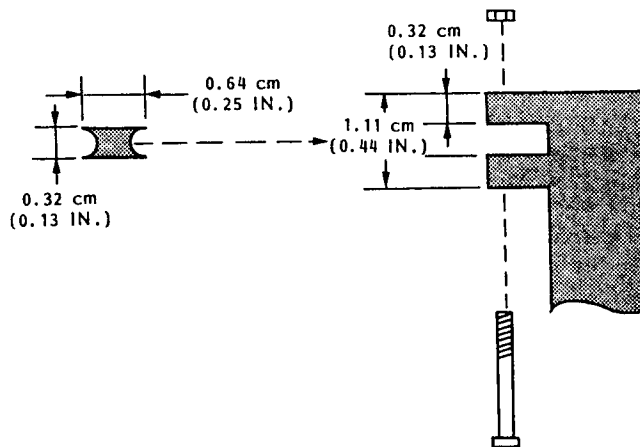


Figure 5. - Exploded view of guide-wire pulley assembly.

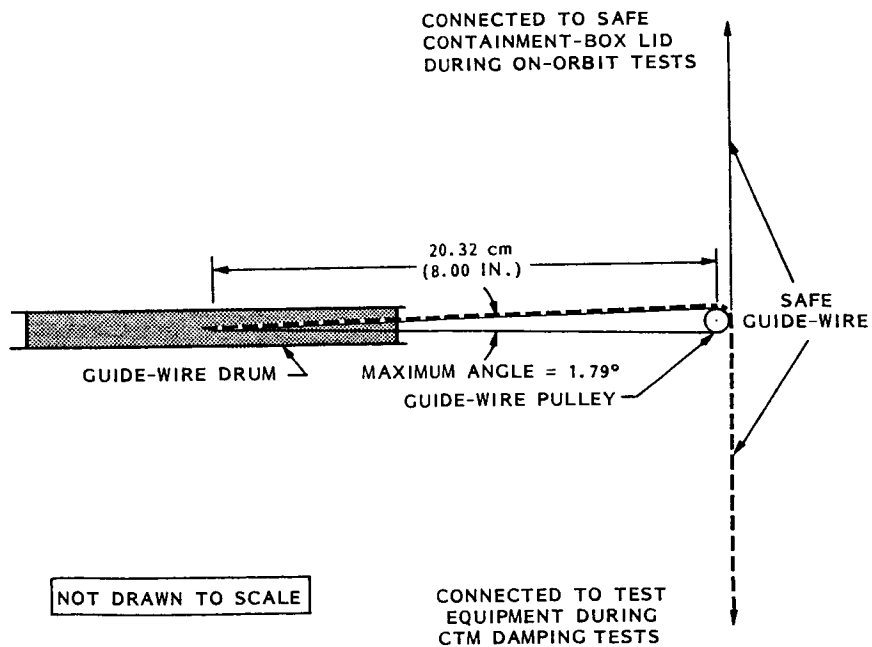


Figure 6. - Guide-wire paths during on-orbit and CTM damping tests.

ORIGINAL PAGE IS  
OF POOR QUALITY



Figure 7. - CTM as installed in SAFE.

ORIGINAL PAGE IS  
OF POOR QUALITY

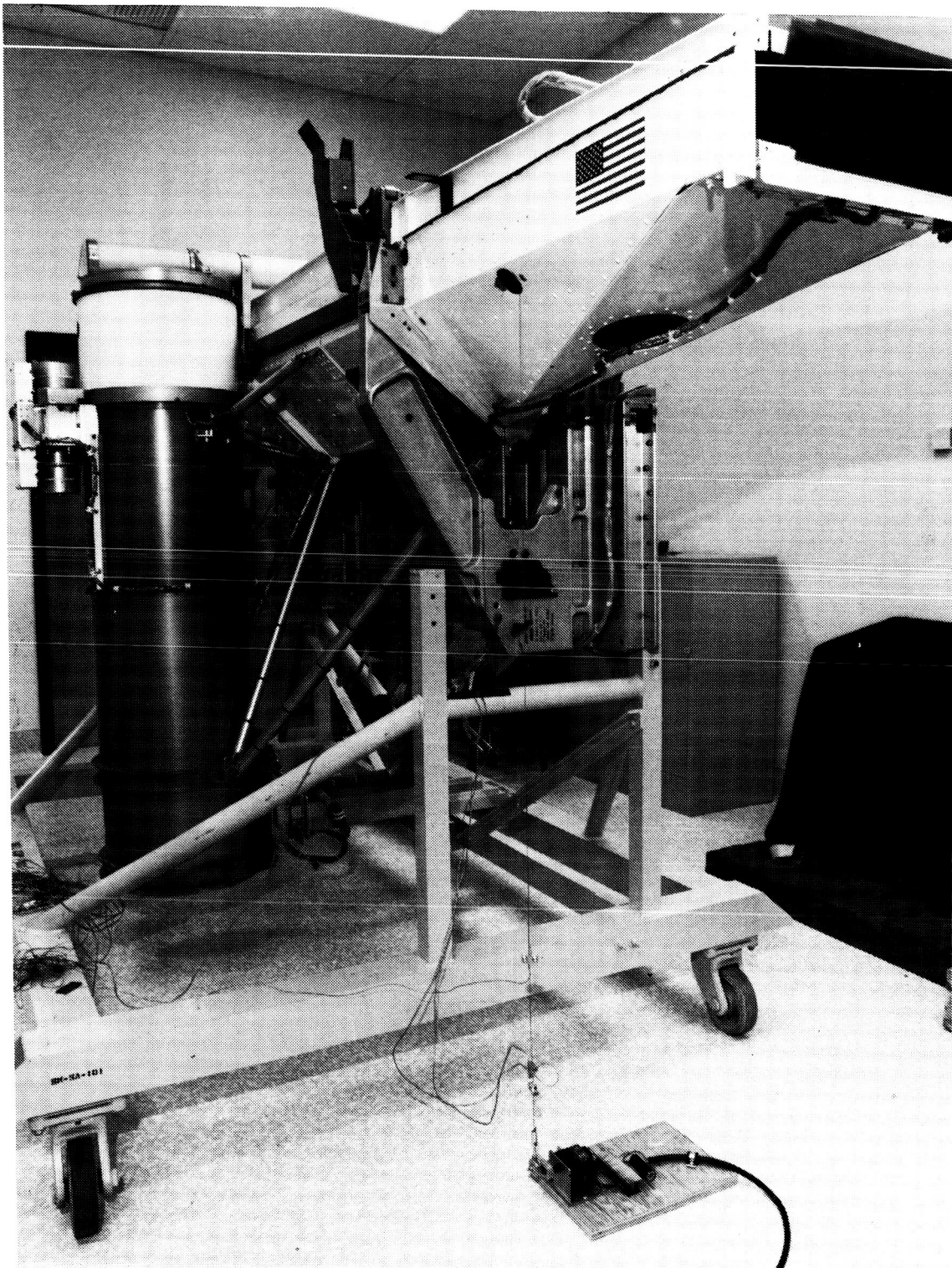


Figure 8. - CTM damping test configuration.